Open Access Library Journal
2024, Volume 11, e11538
ISSN Online: 2333-9721
ISSN Print: 2333-9705

Potential Effects of Climate Trends and Changes on Water and Energy Security in Near-Future Climate Scenarios over Burundi (East Africa)

Célestin Manirakiza, Marc Niyongendako, Prosper Ndizeye, Zénon Nzeyimana

Department of Natural Sciences, Ecole Normale Supérieure of Burundi, Bujumbura, Burundi
Email: manirakiza_celest@yahoo.fr

How to cite this paper: Manirakiza, C., Niyongendako, M., Ndizeye, P. and Nzeyimana, Z. (2024) Potential Effects of Climate Trends and Changes on Water and Energy Security in Near-Future Climate Scenarios over Burundi (East Africa). *Open Access Library Journal*, **11**: e11538.
https://doi.org/10.4236/oalib.1111538

Received: April 5, 2024
Accepted: May 25, 2024
Published: May 28, 2024

Abstract

Climate change is the most dangerous threat facing the world. This article analyzed near-future trends and changes in rainfall, temperature and wind speed over highlands and lowlands of Burundi, and their potential effects on water and electrical energy availability. Observed and gridded data were considered over the period 1981-2020 while forecasts from eight selected CMIP6 models were used over the period 2021-2045. A modified Mann-Kendall's test was used to detect trends while Pettitt's test was adopted to find change points. Future changes in quartiles were analyzed under SSP2-4.5 and SSP5-8.5. The findings revealed upward trends in near-future rainfall all over the study area. In SSP2-4.5, changes of 5.9%, 4.7%, 6.5%, and 5.1% are expected at NHL, NIP, SHL and SIP, respectively. In SSP5-8.5, the increase is projected to reach 10.4% at NHL, 9.7% at NIP, and 10.2% at SHL and SIP. A general increase in temperature is expected all over the study area. The wind speed is predicted to experience an increase of 0.8 $m{\cdot}s^{-1}$ at NHL, NIP and SIP, and 0.7 $m{\cdot}s^{-1}$ at SHL under SSP2-4.5. In SSP5-8.5, the increase will reach 1.0 $m{\cdot}s^{-1}$ at NHL, NIP and SIP, and 0.9 $m{\cdot}s^{-1}$ at SHL by 2045. The detected increase in wind speed is expected to positively impact wind power production and drainage windmills. The increase in rainfall will have positive effects on water availability and hydropower plant production, while higher temperature may increase evaporation and negatively affect water level.

Subject Areas

Atmospheric Sciences

Keywords

Burundi, Climate Change, Climate Trends, Hydropower, Wind Power

1. Introduction

Climate change is a global phenomenon with varying effects from one region to another depending on various socio-economic and environmental factors [1]. Future climate will impact the world in every aspect of life. Climate influences the world through changing temperature, precipitation, snowmelt, and a host of other natural phenomenon [2]. Globally, mean surface air temperature has risen by about 0.74˚C ± 0.18˚C during the twentieth century and is projected to rise by 1.8˚C - 4.0˚C in the twenty-first century [3]. Global extreme precipitation is also projected to increase significantly, especially in regions that are already wet under the current climate conditions, whereas dry spells are predicted to increase particularly in regions characterized by dry weather conditions in the current climate [1]. Furthermore, climate change is predicted to cause stronger surface wind speed values across the boreal regions of the Northern Hemisphere, including much of Canada, Siberia and northern Europe, and in tropical and subtropical regions in Africa, and Central and South America [4]. However, Greenland, southern Europe, China, India, southern Australia and much of the west coast of South America are expected to experience decreasing wind speed values [4] [5].

In East Africa, dry periods are generally associated with La Niña and/or negative Indian Ocean Dipole (IOD) events, while wet periods coincide with El Niño and/or positive IOD events [6]. However, these processes do not explain the full precipitation variability over East Africa. Numerous Global Climate Model (GCM) and Regional Climate Model (RCM) studies project that the East African long rains will increase as they are part of the Intertropical Convergence Zone [7] [8]. However, other studies using regional climate models indicate a reduction in the long rains [9] [10] [11]. This apparent contradiction is leaving the East African rainfall projections more uncertain [9]. Given the recent decline of the long rains, and the current floods reported in many East African countries, people are inevitably wondering what will happen in the next decades, particularly as the climate warms due to continued anthropogenic emissions of greenhouse gases [11]. Furthermore, the Intergovernmental Panel on Climate Change (IPCC) highlighted the need for more detailed information about climate change on regional and local scales, which is of particular interest to nations and economic groups and often dense homogeneous historical datasets are available [1]. The climate in Burundi, as an East African country, is mainly influenced by the North-South movement of the Intertropical Convergence Zone (ITCZ), the topography of the country and El-Niño southern oscillation (ENSO) [12]. However, Burundi has gone through many periods of climatological disasters including droughts, floods, violent winds, and climate related famine [13]. The current crucial challenge is that since 2002, the country has been characterized by a chronic shortage of energy in general and electrical energy in particular [14]. Indeed, Rwegura hydropower plant constructed in September 1986, at the confluence of Kitenge and Mwokora Rivers, has been for many years the main supplier of electric energy within the country. Currently, Rwegura power plant is

facing many problems due to the decrease in rainfall which has resulted in a reduction of water level in the reservoir, creating a decrease in generated power, and this has become an issue of concern [15]. On the other hand, over the last decade, Burundi experienced heavy rainfall causing floods. Furthermore, several projects on hydropower plants are under construction. Consequently, there is a fundamental need to assess the future climate of Burundi, and its potential implications on water and electricity availability. Most of the studies focused on hydrological modeling of Rwegura catchment [16], but they did not address trends and changes in rainfall, temperature and wind speed over the highlands and western lowlands, and their potential effects on water and energy security. Therefore, this article aims to fill that gap. Specifically, the study focuses on evaluating current trends (1981-2020) in rainfall, temperature and wind speeds, and their changes over the near-future period (2021-2045) referring to the new climate normal (1991-2020). It discusses at the same time the effects of the detected trends and changes on water and electrical energy availability.

2. Materials and Methods

2.1. Study Area

Figure 1 locates the study area in Burundi. Burundi is an East African country ranging between longitudes 28.8˚ and 30.9˚ East, and latitudes 2.3˚ and 4.45˚ South [17].

Bounded to the north by Rwanda, to the East and South by Tanzania and to the West by the Democratic Republic of Congo (DRC), Burundi covers an area of 27834 km^2 [18]. The annual rainfall in the high altitude regions is almost the double that of low altitudes. Average maximum annual temperatures range from 21.8˚C to 29.5˚C. The average wind speeds vary between 4 $m{\cdot}s^{-1}$ and 6 $m{\cdot}s^{-1}$ [19]. The considered study sites are highlands and western lowlands of Burundi. The highlands elevation is between 1750 and 2650 m altitude while lowlands are between 770 and 1100 m altitude. For better analysis, the highlands were divided into Northern Highlands (NHL) and Southern Highlands (SHL) while the Western lowlands were split into Northern Imbo Plain (NIP) and Southern Imbo Plain (SIP) as in Manirakiza *et al.* [20].

2.2. Data Source

2.2.1. Observed Dataset

Two sets of data are used in this study as observed data. The first set consists of *in-situ* data collected from the synoptic stations of Burundi belonging to the Geographical Institute of Burundi (IGEBU). **Figure 1** locates the nineteen meteorological stations used, while **Table 1** gives their concise information. Rainfall, temperature and wind speed observed data were collected at daily scale over the period 1981-2020. Indeed, among the nineteen climate stations, six had shorter period than the normal of 30 years recommended by World Meteorology Organization (WMO) for a climate study.

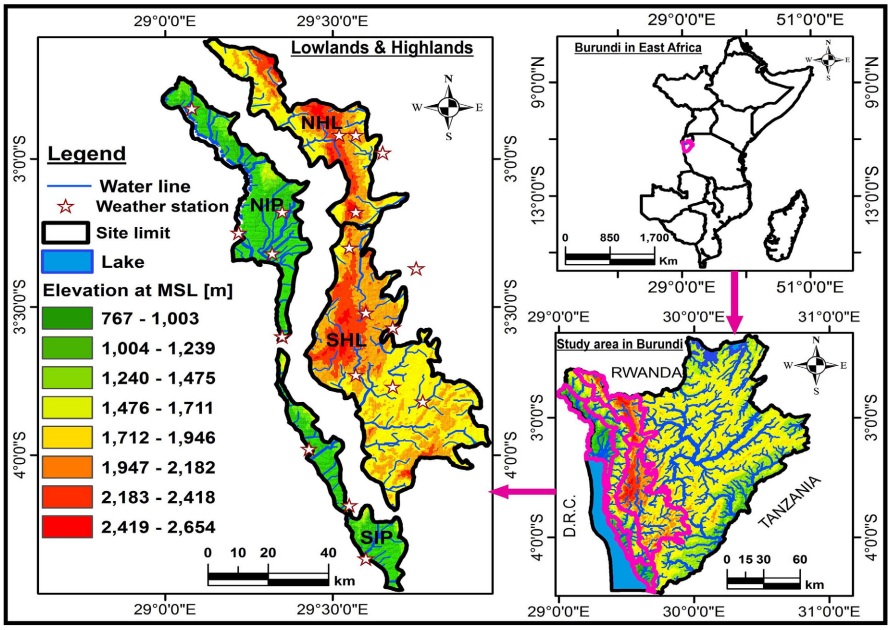

Figure 1. Study area location.

Table 1. Geographic characteristics of the meteorological stations used.

Site	Station name	ID (IGEBU)	Longitude	Latitude	Period	T[a] (%)	Alt.[b]
NHL	Munanira	10106	29.57	−2.92	1981-2002	55	2120
	Rwegura	10164	29.52	−2.92	1981-2020	100	2302
	Gatara	10036	29.65	−2.98	1981-1994	35	1806
	Teza	10167	29.57	−3.18	1981-2020	100	2166
	Bugarama	10003	29.55	−3.3	1981-2020	100	2240
SHL	Gisozi	10044	29.68	−3.57	1981-2020	100	2097
	Mpota	10098	29.57	−3.73	1981-2020	100	2160
	Kibumbu	10068	29.75	−3.37	1981-2020	100	1814
	Nyakararo	10141	29.6	−3.52	1981-2020	100	2228
	Matana	10089	29.68	−3.77	1981-2020	100	1934
	Ruvyironza	10161	29.77	−3.82	1981-2020	100	1822
NIP	Mutumba	10123	29.35	−3.6	1981-2000	50	971
	Bujumbura	10011	29.32	−3.32	1981-2020	100	783
	Imbo	10052	29.35	−3.18	1981-2020	100	820
	Mparambo	10095	29.08	−2.83	1981-2020	100	887
	Rukoko	10151	29.22	−3.25	1981-1995	37.5	790
SIP	Kigwena	10074	29.55	−4.17	1981-1997	42.5	914
	Rumonge	10152	29.43	−3.98	1981-1987	17.5	785
	Nyanza Lac	10145	29.6	−4.35	1981-2020	100	792

[a]T = Time period in percentage included in the period of study. [b]Alt. = Altitude in meters.

To complement *in-situ* observed values, the second set of gridded data was used. In fact, gridded daily precipitation from Climate Hazards group Infrared Precipitation with Stations (CHIRPS) downloaded from https://cds.climate.copernicus.eu/ and monthly temperature data from Climate Research Unit (CRU TS 4.01) available online at https://crudata.uea.ac.uk/cru/data/hrg/ were used to complement *in-situ* rainfall and temperature, respectively. In addition, MERRA-2 (Modern Era Reanalysis for Research and Applications Version 2) hourly wind speed data available online at https://gmao.gsfc.nasa.gov/reanalysis/MERRA-2/ were used to complement *in-situ* wind speed. The gridded data set is very useful in view of the fact that weather stations are limited in number, unevenly distributed, have missing data problem and short period of observation [21]. The selection of the time series data from various stations was based on the quality control using the same procedure as in Javier *et al.* [22], while the cross validation method following Ioannis [23] was adopted to fill missing data. **Figure 2** shows the correlations [r] in (a) between CHIRPS and *in-situ* data, in (b) between CRU and *in-situ* data, and in (c) between MERRA-2 and *in-situ* data. Indeed, (a) has the strongest correlation. Overall, the three subfigures show that the gridded data used are very strongly correlated to *in-situ* data with correlation coefficients greater than 0.86.

Overall, **Table 2** presents the statistical summary of the used data at annual scale.

2.2.2. CMIP6 Model

This third set of used data is made of daily rainfall, temperature (tas) and wind speed (WS) from eight Climate Models over the period 1981-2045. These data are available in the context of the Coupled Model Intercomparison Project Phase six (CMIP6) and accessed online (https://esgf-node.llnl.gov/search/cmip6) through user registration. **Table 3** shows the used climatic models where the second column gives their acronyms adopted in this paper. CMIP6 models have already been used over East Africa [24] and particularly over Burundi [25] for climate projection. CMIP6 uses Shared Socio-economic Pathways (SSPs) which are considered as more realistic future scenarios [26]. In this paper, two experiments performed respectively under the medium and the strong forcing Shared Socio-economic Pathway scenarios namely SSP2-4.5 and SSP5-8.5 have been adopted for the near-future projection (2021-2045). The SSP2-4.5 scenario is referred to as a more plausible outcome where modest mitigation implementation will curb the global warming to about 2.5˚C warming relative to pre-industrial period by the end of the 21st century [27]. On the other hand, the SSP5-8.5 is considered as "business as usual", implying a dystopian future that is fossil-fuel intensive, void of stringent climate mitigation, leading to nearly 5˚C of warming by 2100 [24]. The detail description of used scenarios is available in Riahi, K. *et al.* [27]. This most up-to-date set of data was at different horizontal resolutions. Using the same technique as in Iturbide *et al.* [28], we regridded all CMIP6 data from original spatial resolutions to 0.05˚ × 0.05˚ common grid resolution to

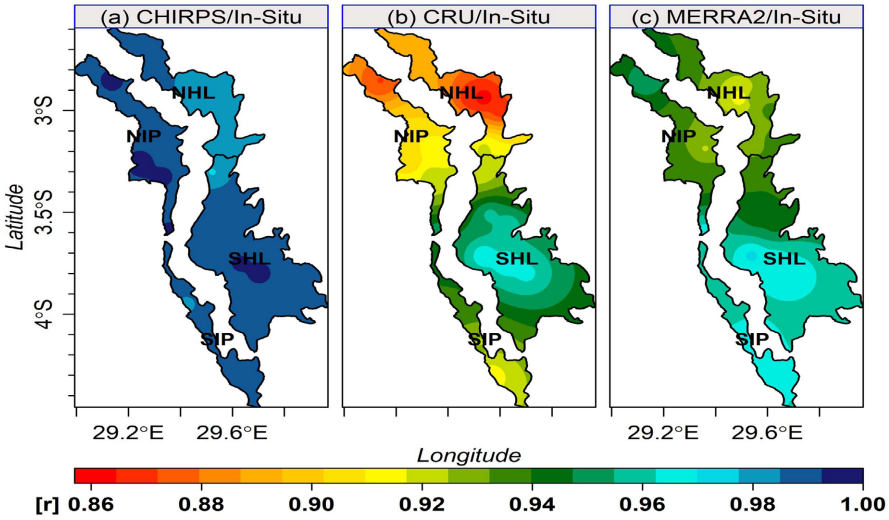

Figure 2. Correlation between *in-situ* data and gridded data used.

Table 2. Description of data collected over the period 1981-2020 at annual scale.

Variable	Site	Minimum	Maximum	Mean	Standard deviation
Rainfall (mm)	NHL	1249.6	1921.1	1493.3	158.3
	NIP	693.8	1148.6	899.1	108.9
	SHL	1133.8	1756.3	1435.5	155.9
	SIP	982.2	1396.1	1203.4	103.8
tas[1]	NHL	15.7	16.8	16.3	0.3
	NIP	23.2	25.2	24.2	0.4
	SHL	15.5	17.1	16.5	0.4
	SIP	22.8	24.1	23.5	0.3
WS[2]	NHL	3.8	5.2	4.4	0.3
	NIP	3.6	4.7	4.2	0.3
	SHL	3.3	4.7	3.9	0.3
	SIP	3.7	5.7	4.7	0.4

[1]tas = Mean temperature in (˚C); [2]WS = Wind speed in ($m \cdot s^{-1}$).

Table 3. Climatic models used.

CMIP6 Model Name	Model Short Name	Origin Country	Resolution	Variant label
ACCESS-ESM1-5	ACCESS	Australia	1.9˚ × 1.2˚	r1i1p1f1
CanESM5	CanESM5	Canada	2.8˚ × 2.8˚	r1i1p1f1
CESM2-WACCM	CESM2	USA	1.3˚ × 0.9˚	r1i1p1f1
CNRM-CM6-1	CNRM	France	1.4˚ × 1.4˚	r1i1p1f2
FGOALS-f3-L	FGOALS	China	1.3˚ × 1˚	r1i1p1f1
IPSL-CM6A-LR	IPSL	France	2.5˚ × 1.3˚	r1i1p1f1
MIROC-ES2L	MIROC	Japan	2.8˚ × 2.8˚	r1i1p1f2
NorESM2-MM	NorESM2	Norway	0.9˚ × 1.25˚	r1i1p1f1

match with the highest resolution of CHIRPS data. For more accuracy and better analysis, a Multi-Model Ensemble (MME) has been computed from the eight climate models. Moreover, CMIP6 data have been downscaled at climate stations using Empirical Statistical Downscaling [29] and bias adjusted using Quantile Delta Mapping approach [30]. Furthermore, the data on WS presented in **Table 2** were collected at 12 m height. However, CMIP6 WS data were at 10 m height, and the power law was used for extrapolation at 12 m height as in Lawin *et al.* [31].

2.3. Methods

2.3.1. Variability Analysis

For each variable, surplus months/years and deficit months/years are determined using the standardized variable index (I) developed by Mckee *et al.* [32] which can be found in many articles [18] [20]:

$$I(i)=\frac{X_i-\bar{X}_m}{\sigma}$$

where X, $\bar{X}_m$ and σ are respectively the value for the month/year *i*, the average and the standard deviation of the time series. In this study, a month/year is considered normal if its index is included between −0.5 and +0.5. It is in surplus if its index is greater than +0.5 and in deficit below −0.5. This interval is questionable since it is relatively small. However, it can single out well deficit months/years from surplus months/years.

2.3.2. Trend Analysis

The trend analysis was carried out over three time periods including 1981-2010, 1981-2020 and 1991-2020. In this regard, the Mann-Kendall's (MK) test (1945) [33] [34] remains a robust and popular choice for researchers. However, the Power of Mann-Kendall's test is highly influenced by serially correlated data. To address this issue, a modified Mann-Kendall (MMK) trend test applied to Trend-Free Pre-Whitened time series data in presence of serial correlation (TFPWMK test) following Yue *et al.* [35] approach has been adopted in this study. In addition, whenever a MMK's trend was not significant at the chosen threshold of 0.05, the Theil-Sen median slope trend analysis, which is a linear trend calculation that is resistant to the impact of outliers (noise) [36] was utilized for trend estimate. Furthermore, the Pettitt's test (1979) [37] has been applied for break point detection. All these tests are worldwide used in hydro meteorological variables trend analysis [21] [38].

2.3.3. Future Change Analysis

Future changes are analyzed over the period 2021-2045 based on CMIP6 scenarios, here SSP2-4.5 and SSP5-8.5, referring to the most recent normal period 1991-2020 as recommended by WMO. For rainfall and WS, the change is computed as the ratio between the future climate scenario and the current climate, while the change for the tas was respectively calculated as the difference between

the two climates. Changes in quartiles are analyzed for each climate model using violins as in manirakiza *et al.* [20]. On the other hand, the spatial distribution of changes has been mapped using Inverse Distance Weighted (IDW) interpolation method [39].

3. Results and Discussion

3.1. Trends Analysis over the Current Climate

3.1.1. Seasonal Rainfall

Figure 3 presents the monthly standardized rainfall at NHL, NIP, SHL and SIP over the period 1981-2020. The findings show that the months 6 and 8 are normal all over the study area. September (9) is also normal over the study area, except at NHL where it is in excess rainfall. July (7) is normal at NIP and SIP, while it is in deficit rainfall at NHL and SHL. These months of low rainfall correspond to the dry season in Burundi. During this season, hydropower plants experience the decrease of the water level in the reservoir which leads to difficult hydropower rationing [15].

The analysis also shows the months 1, 2, 3, 4, 5, 10, 11 and 12 to be in excess rainfall all over the four sites. July was pointed out as a month with the lowest amount of rainfall all over the four sites, while April is the wettest at NHL, SHL and SIP. At NIP, December (12) was singled out as the wettest month. Overall, eight months in excess rainfall were found at NIP, SHL and SIP, while 9 months in excess rainfall were noticed at NHL, respectively.

3.1.2. Interannual Rainfall

Figure 4 depicts the interannual rainfall at NHL, NIP, SHL and SIP over the period 1981-2020. The analysis of the standardized rainfall index shows 13 years in deficit rainfall at NHL and NIP, while SHL and SIP have 16 and 11 years in deficit rainfall, respectively. From 1981 to 2020, the features revealed 10, 12, 11 and 15 years in excess rainfall at NHL, NIP, SHL and SIP, respectively. For trend detection, over the period 1981-2010, MMK's test using the TFPWMK approach detected a significant decreasing trend at NHL and SIP, where Kendall's tau equal to −0.35 and −0.28 with p-value of 0.007 and 0.03, respectively were estimated. Indeed, Pettitt's test revealed only a significant change point in 1991 at SIP with a p-value of 0.022. The analysis showed a decrease of 120 mm in average annual rainfall over the sub period after the break point. Furthermore, Sen's slope estimated a downward trend at NIP and SHL with −1.37 and −3.39, respectively.

Overall, the period 1981-2010 is characterized by a downward trend in rainfall which has negative effects on water availability and hydropower production [15] [18]. Over the period 1981-2020, MMK's test detected no significant trend all over the study area at threshold of 0.05. On the other hand, Pettitt's test only singled out significant break points at NIP in 2008 and at SHL in 2010 with respective p-values of 0.028 and 0.019. The analysis revealed respectively an

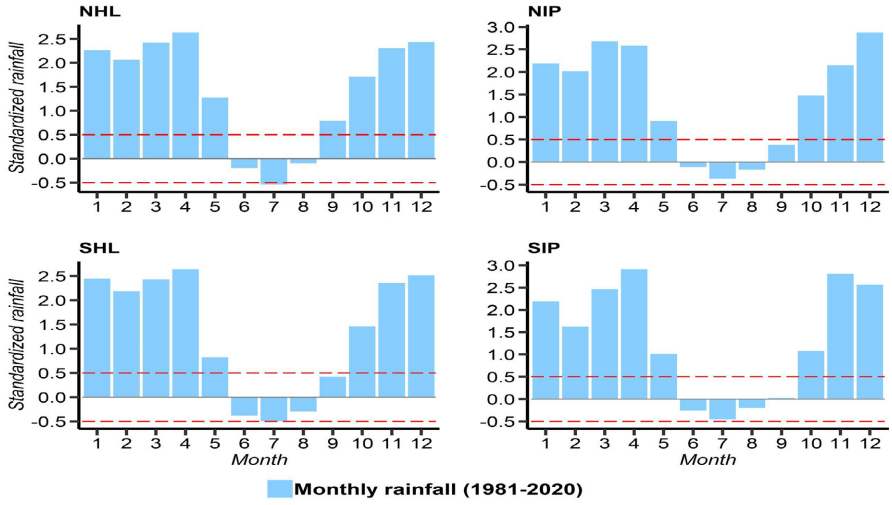

Figure 3. Monthly standardized rainfall at NHL, NIP, SHL and SIP over the period 1981-2020.

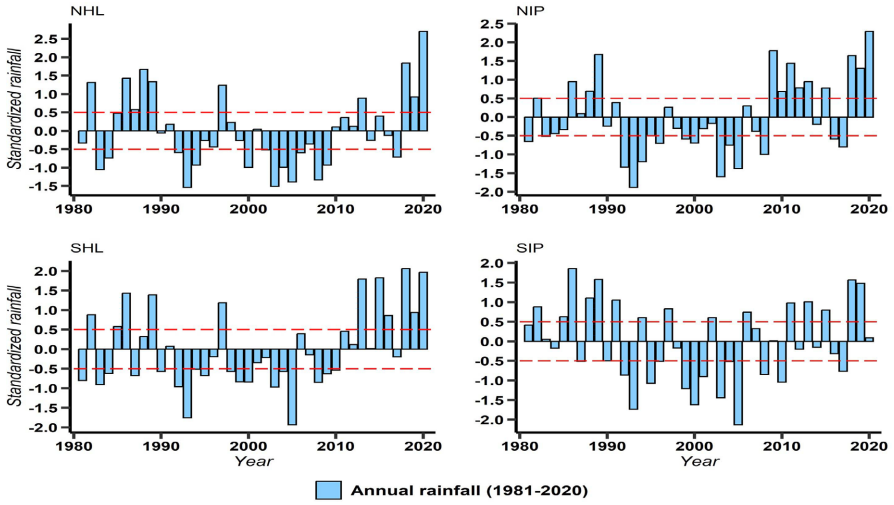

Figure 4. Interannual standardized rainfall at NHL, NIP, SHL and SIP over the period 1981-2020.

increase of 131 mm and 161 mm in average annual rainfall at NIP and SHL over the sub period after the change point. Moreover, Sen's slope estimated an upward trend respectively at NHL, NIP and SHL with 0.83, 2.64 and 4.16, while a downward trend was estimated at SIP with −0.05. Over the period 1991-2020, MMK's test detected a significant increasing trend all over the study area, where Kendall's tau equal to 0.39, 0.48, 0.47 and 0.28 with p-value of 0.0032, 0.0002, 0.00034 and 0.03403 were respectively estimated at NHL, NIP, SHL and SIP. Moreover, Pettitt's test revealed significant change points in 2009, 2008 and 2010 with p-value of 0.0148, 0.0046 and 0.0030 estimated at NHL, NIP and SHL, respectively. The analysis showed respectively an increase of 181 mm, 163 mm and 238 mm in average annual rainfall at NHL, NIP and SHL over the sub period after the change point. Overall, this upward trend in rainfall over the most recent normal period is consistent with the findings in many studies from East Africa

[8] [26] [38] and what has been experienced in Burundi over the last decade. This new trend has a positive impact on water availability and hydropower production.

3.1.3. Seasonal Temperature

Figure 5 depicts the monthly standardized tas at NHL, NIP, SHL and SIP over the period 1981-2020.

The findings point out July as the coolest month while September is the hottest. In fact, in July, NIP showed the lowest value equal to −2.5 while in September, SIP revealed the highest value equal to 1.6. Furthermore, the features revealed 3 months of excess tas at NHL and NIP while at SHL and SIP, the findings highlighted respectively 5 and 2 months in excess tas. Moreover, the months 6 and 7 are cool at NHL, SHL and SIP while at NIP the month 8 is also included as cool. The analysis noticed that at NHL and SIP, September and October have the same value.

3.1.4. Interannual Temperature

Figure 6 shows interannual standardized tas at NHL, NIP, SHL and SIP over the period 1981-2020. The analysis revealed 9 years in low tas at NHL, NIP and SHL, while SIP has 10 years in low tas. The features also pointed out 10 years in high tas at NHL and SHL, while 11 years were detected at NIP and SIP. Indeed, over the period 1981-2010, MMK's test detected a significant increasing trend in tas at NHL, NIP, SHL and SIP, where Kendall's tau equal to 0.3473, 0.6084, 0.4778 and 0.3399 with p-values equal to 0.0086, 0.0000, 0.0003 and 0.0102 were respectively estimated. Moreover, Pettitt's test revealed a significant change point in 1996 at NHL, NIP, SHL and SIP with respective p-values of 0.0087, 0.001, 0.0071 and 0.0087. The analysis revealed an increase of 0.31˚C, 0.59˚C, 0.41˚C and 0.36˚C over the sub period after the break point at NHL, NIP, SHL and SIP, respectively. Over the period 1981-2020, MMK's test revealed a significant increasing trend in tas at NHL, NIP, SHL and SIP, where Kendall's tau equal to 0.406, 0.555, 0.377 and 0.379 with p-values equal to 0.0003, 0.0000, 0.0008 and 0.0007 were respectively estimated.

On the other hand, Pettitt's test singled out significant break points in 2000 at NHL, in 2002 at NIP, in 1996 at SHL and SIP with respective p-values of 0.0006, 0.0000, 0.0050 and 0.0009. The analysis revealed an increase in tas over the sub period after the change point of 0.33˚C, 0.59˚C, 0.41˚C and 0.36˚C at NHL, NIP, SHL and SIP, respectively. Over the period 1991-2020, MMK's test detected a significant increasing trend in tas at NHL and NIP, where Kendall's tau equal to 0.310 and 0.300 with p-values of 0.0190 and 0.0232 were respectively estimated. Moreover, Pettitt's test singled out significant change points only in 1992 at NIP, and in 1994 at NHL and SIP with respective p-values of 0.0057, 0.0180 and 0.0353. The analysis revealed an increase of 0.27˚C, 0.59˚C and 0.30˚C in tas at NHL, NIP and SIP over the sub period after the change point, respectively. On the other hand, MMK's test detected no significant trend at SHL and SIP, while

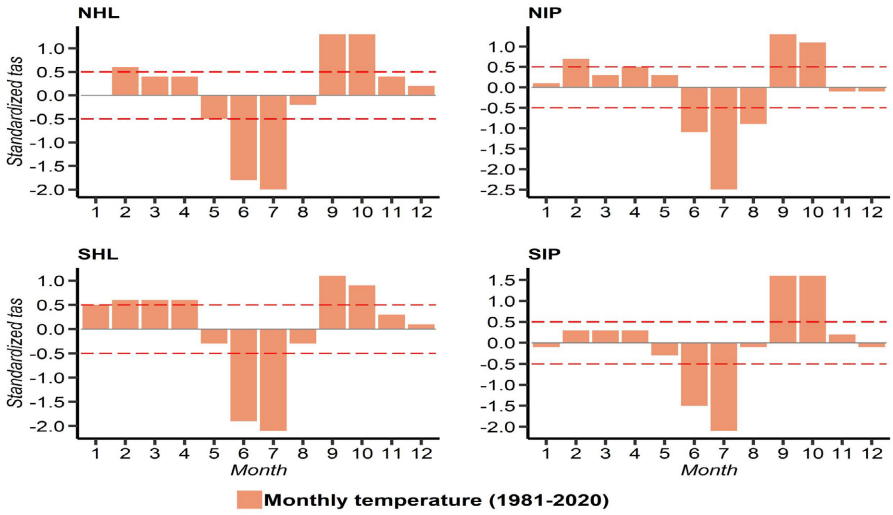

Figure 5. Monthly standardized tas at NHL, NIP, SHL and SIP over the period 1981-2020.

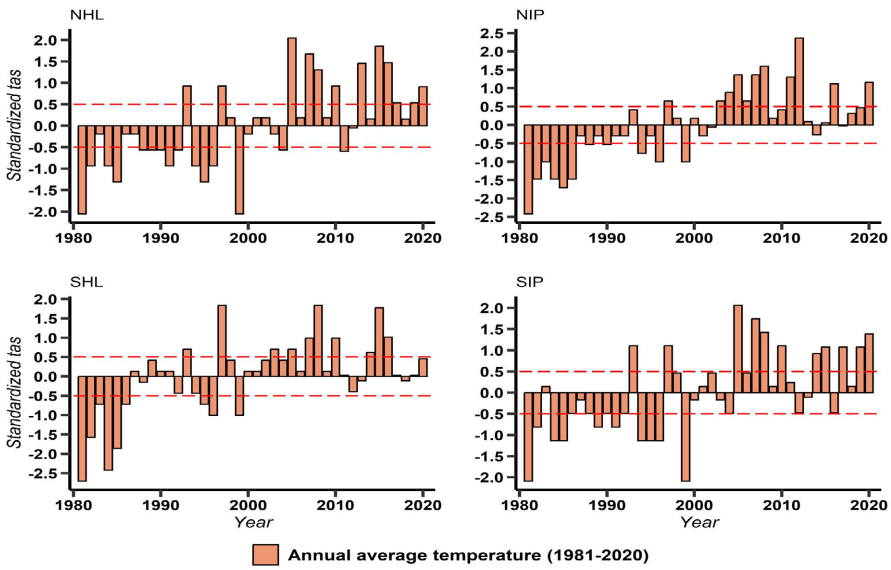

Figure 6. Interannual standardized tas at NHL, NIP, SHL and SIP over the period 1981-2020.

Sen's slope estimated an upward trend at SHL and SIP with 0.0066 and 0.0145, respectively. These findings are in accordance with the findings in many studies which show increasing in temperature over the last century due to climate warming [15] [21] [26]. Consequently, high temperatures may increase evaporation and reduce water availability [18].

3.1.5. Monthly Wind Speed and Wind Direction

Figure 7 depicts the standardized WS and diurnal wind direction at monthly scale over the period 1981-2020 across NHL, NIP, SHL and SIP. The analysis of the WS shows two parts including months of low WS and months of high WS. In fact, the findings showed that at NHL, NIP, SHL and SIP, the months

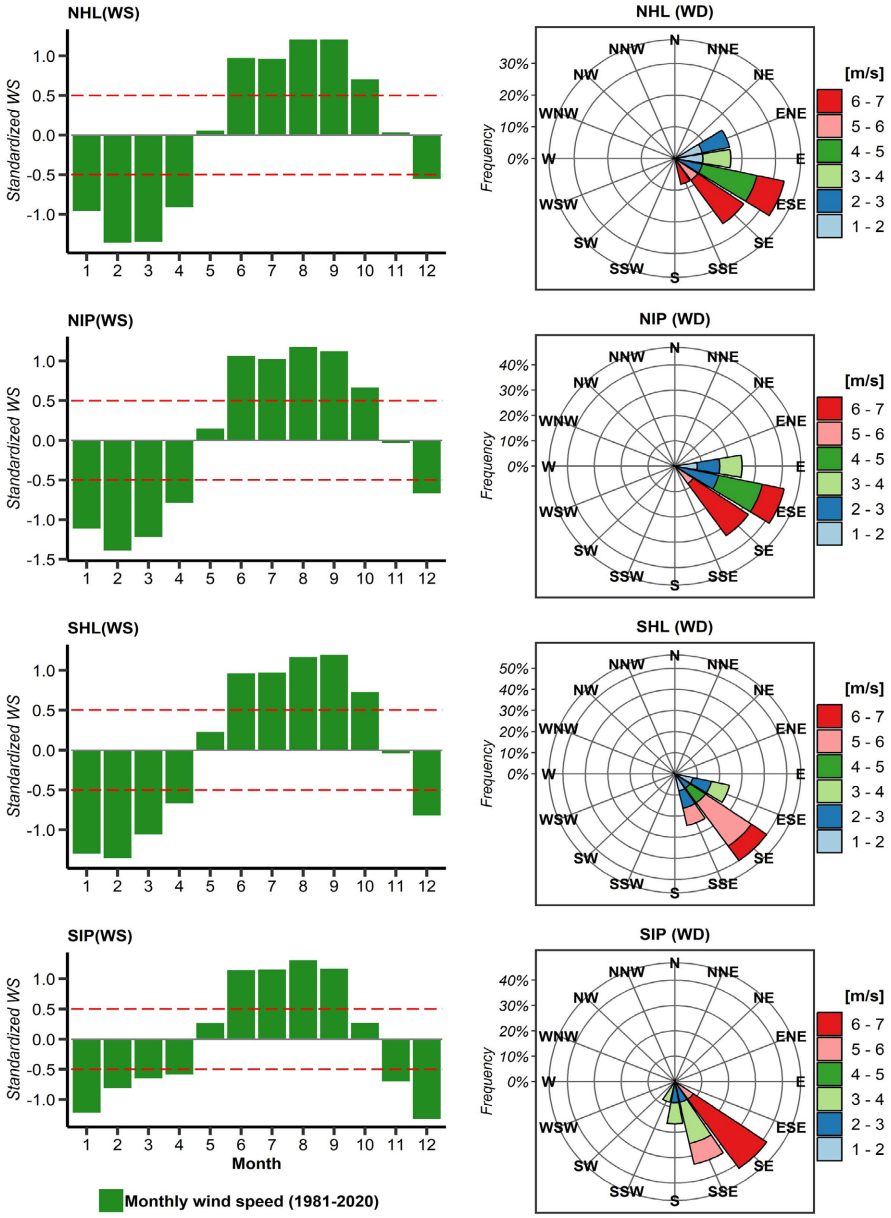

Figure 7. Monthly standardized WS and average wind direction over the period 1981-2020.

1, 2, 3, 4 and 12 have low WS, while the months 6, 7, 8, and 9 have high WS. In addition, October has high WS at NHL, NIP and SHL, while November has low WS at SIP. The analysis of **Figure 3** and **Figure 7** shows that this period of upward trend in WS matches with dry season in Burundi in general and in particular at the study area, where rainfall records the decrease.

These findings are in accordance with those by Lawin *et al.* [18] and Manirakiza *et al.* [20] who reported that mean WS are optimized during summer time and that this may reveal the period when wind power turbines would expect receiving maximum WS in Burundi. On the other hand, the analysis of the right features on wind direction (WD) reveals that at NHL and NIP, the prevailing

winds blow from East-South-East (ESE). Indeed, at NHL, the wind blowing with the highest speeds (between 6 and 7 $m \cdot s^{-1}$) is from ESE with a frequency of 8%, South-East (SE) with a frequency of 18% and South-South-East (SSE) with a frequency of 8%. At NIP, the wind blowing with the highest speeds (between 6 and 7 $m \cdot s^{-1}$) is from ESE and SE with a frequency of 7.5% and 25%, respectively. Furthermore, the analysis of spokes shows that at SHL and SIP, the prevailing winds blow from SE. Indeed, at SHL and SIP, the wind blowing with the highest speeds (between 6 and 7 $m \cdot s^{-1}$) is from SE with a frequency of 10% and 35%, respectively.

3.1.6. Interannual Wind Speed

Figure 8 shows interannual standardized WS at NHL, NIP, SHL and SIP over the period 1981-2020. The analysis singled out two main parts. The first part includes the period 1981-1996 with many years in low WS, while the second part includes the period 1997-2020 with many years in high WS. In fact, at NHL, the first part has 8 years in low WS with 1 year in high WS, while the second part revealed 10 years in high WS with 2 years in low WS. At NIP, the first part revealed 10 years in low WS with no year in high WS, while the second part has 11 years in high WS with 2 years in low WS.

At SHL, the first part has 8 years in low WS with no year in high WS, while the second part revealed 10 years in high WS with 2 years in low WS. Furthermore, at SIP, the first part revealed 11 years in low WS with no year in high WS, while the second part has 9 years in high WS with 2 years in low WS. On the other hand, over the period 1981-2010, MMK's test using the TFPWMK approach revealed a significant upward trend in average WS at NHL, NIP, SHL and SIP, where Kendall's tau equal to 0.3498, 0.4828, 0.3842 and 0.3300 with p-values equal to 0.0082, 0.0003, 0.0036 and 0.0126 were respectively estimated. Moreover, Pettitt's test pointed out a significant change point in 1996 with p-values of 0.0093 at NHL, 0.0005 at SIP, and 0.0002 at NIP and SHL. The analysis revealed an increase in average WS over the sub period after the change point of 0.4 $m \cdot s^{-1}$ at NHL and SIP, and 0.3 $m \cdot s^{-1}$ at NIP and SHL. Overall, the detected upward trend over the period 1981-2010 is consistent with many findings on East Africa in general and particularly on Burundi [20] [31] as effects of climate change. Over the period 1981-2020, MMK's test revealed a significant upward trend in average WS at NHL, NIP, SHL and SIP, where Kendall's tau equal to 0.3495, 0.4440, 0.4656 and 0.5412 with p-values equal to 0.00180, 0.00007, 0.00003 and 0.00000 were respectively estimated. Moreover, Pettitt's test detected a significant break point in 1996 with p-values of 0.0072 at NHL, 0.0003 at NIP and SHL, and 0.0000 at SIP. The analysis highlighted an increase of 0.3 $m \cdot s^{-1}$ at NHL and NIP, 0.4 $m \cdot s^{-1}$ at SHL, and 0.6 $m \cdot s^{-1}$ at SIP in average annual WS over the sub period after the break point. Over the period 1991-2020, MMK's test detected a significant increasing trend in average WS at NIP, SHL and SIP, where Kendall's tau equal to 0.3892, 0.3695 and 0.5567 with p-values of 0.0032, 0.0052 and 0.0000 were respectively estimated. MMK's test detected no

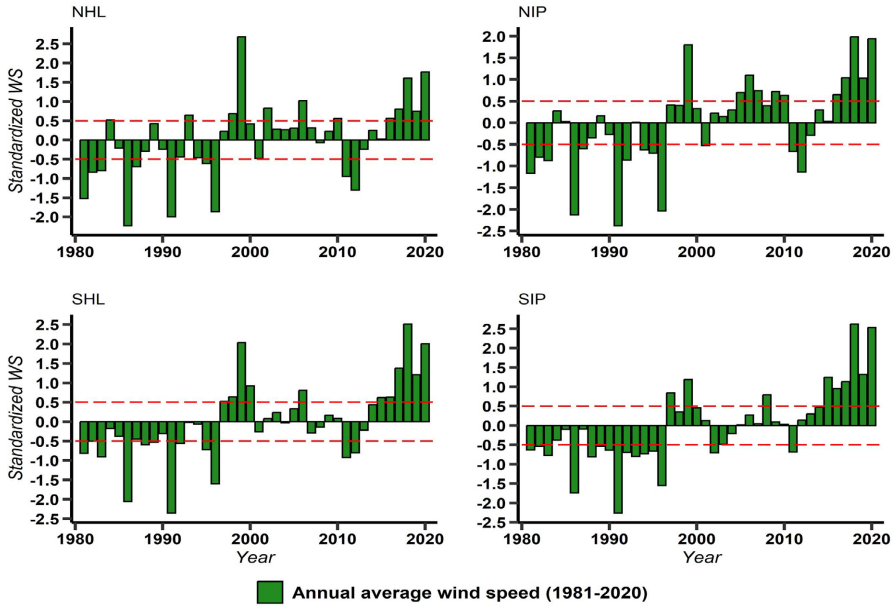

Figure 8. Interannual standardized WS at NHL, NIP, SHL and SIP over the period 1981-2020.

significant increasing trend at NHL, while Sen's slope estimated the upward trend in average WS at NHL with 0.0110. On the other hand, Pettitt's test only revealed a significant change point in 2011 at SIP with a p-value of 0.0100. Indeed, the analysis singled out an increase in average WS of 0.6 $m \cdot s^{-1}$ at SIP over the sub period after the change point. The upward trend in WS found over the four sites may have positive impact on wind power production, and hence reduce the electrical gap observed during the long dry season or be used for water pumping in the irrigation system.

3.2. Future Change Analysis

3.2.1. Projected Rainfall and Changes

Figure 9 compares the projected monthly rainfall by the MME under SSP2-4.5 and SSP5-8.5 over the period 2021-2045 with those over the baseline period 1991-2020.

The analysis reveals that at NHL, the monthly rainfall is projected to increase in June-February, while March-May is predicted to experience the decrease in rainfall under SSP2-4.5. Following SSP5-8.5, an increase in rainfall is expected in June-March, while a decrease is projected in April and May. At NIP, the monthly rainfall is expected to increase in August-February, while the months March-July are projected to experience the decrease in rainfall under SSP2-4.5. Moreover, under SSP5-8.5, the rainfall is expected to increase in June-February, while a decrease is predicted in March-May. At SHL, the monthly rainfall is predicted to increase in May-March, while a decrease in rainfall is expected in April under both scenarios. At SIP, the monthly rainfall is expected to increase in August-October and December-February, while November and March-July are predicted to experience the decrease in rainfall under SSP2-4.5. Indeed, under

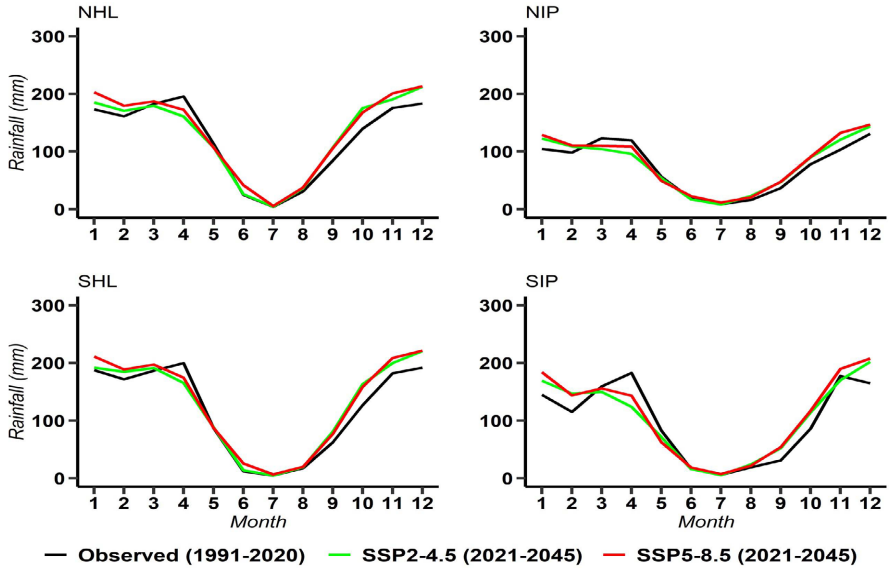

Figure 9. Projected monthly rainfall over the period 2021-2045.

SSP5-8.5, the rainfall is projected to increase from June to February, while a decrease is expected in March-May. Overall, the analysis highlighted that several months are expected to increase in rainfall all over the four sites. For future trend analysis, **Figure 10** uses violins to explain the projected rainfall changes at annual scales.

The red dot shows the rainfall change projected by the MME. The thicker part indicates that the rainfall change value in that section of the violin has higher frequency, and the thinner part implies lower frequency. For more clarity, only models corresponding to the maximum and minimum changes have been visualized with the violin. Furthermore, changes are analyzed within quartiles. Therefore, the first crossbar of the violin marks the 1st quartile, the second crossbar is the 2nd quartile (median) and the last is the 3rd quartile. Indeed, the figure shows that in SSP2-4.5, the rainfall increase equal to 5.9%, 4.7%, 6.5% and 5.1% is expected at NHL, NIP, SHL and SIP, respectively. In the same way, following SSP5-8.5, it is predicted an increase in rainfall equal to 10.4% at NHL, 9.7% at NIP, and 10.2% at SHL and SIP. The findings highlighted that SHL and NHL are projected to experience the highest increase in rainfall under SSP2-4.5 and SSP5-8.5, respectively. Furthermore, the rainfall increase will be higher in the highlands than lowlands. Meanwhile, the maximum rainfall change is projected by CESM2 model all over the four sites under SSP2-4.5 and SSP5-8.5. On the other hand, the minimum rainfall change is projected by NorESM2 and MIROC under SSP2-4.5 and SSP5-8.5, respectively. The analysis of changes in quartiles reveals that models' rainfall change values have the higher frequency in the first and second quartiles for SSP2-4.5 and in the second and third quartiles for SSP5-8.5. Overall, the predicted increase in annual rainfall found in this study will have effects on water availability. This may include the water level change in the Lake Tanganyika. Indeed, as Burundi hydropower production is

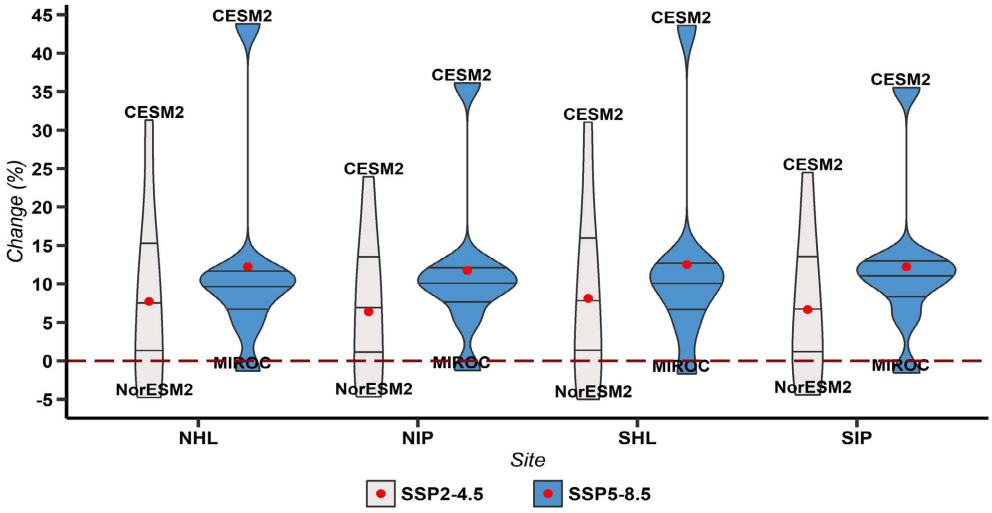

Figure 10. Projected changes in annual rainfall over the period 2021-2045.

dependent on rainfall, the increase in rainfall will positively affect hydropower plants located in the study area. Similar to other regional studies [9] [38], our findings predict that over the period 2021-2045, annual rainfall trends will increase.

3.2.2. Projected Temperature and Changes

Figure 11 depicts the projected monthly average temperature by the MME at NHL, NIP, SHL and SIP under SSP2-4.5 and SSP5-8.5 over the period 2021-2045.

The analysis highlights a general increase in monthly tas all over the four sites by 2045. Indeed, the month of July is expected to experience the highest increase all over the study area with values equal to 1.9˚C at NHL, 2˚C at NIP and SHL, and 2.4˚C at SIP under SSP2-4.5, while following SSP5-8.5 these values are forecasted to reach 2.4˚C, 2.6˚C, 2.3˚C and 2.7˚C at NHL, NIP, SHL and SIP, respectively. The findings showed that months which were currently the coolest are expected to experience the highest increase in tas by 2045. Indeed, the projected increase in tas will have effect on lifestyle of the population. It may also increase water evaporation especially in the Lake Tanganyika between Burundi, DRC, Zambia and Tanzania. On the other hand, **Figure 12** shows annual tas changes in quartiles. In fact, in SSP2-4.5, it is projected changes in tas equal to 0.8˚C at NHL and SHL, and 1˚C at NIP and SHL.

Under SSP5-8.5, the changes in tas will reach 1.1˚C at NHL and SHL, and 1.2˚C at NIP and SIP. Furthermore, the minimum change is projected by CESM2 all over the four sites under both SSP2-4.5 and SSP5-8.5. On the other hand, the maximum change in tas is forecasted by CanESM5 all over the four sites in both scenarios except at NHL and SHL in SSP5-8.5, where NorESM2 projected the maximum changes. Overall, sites which were currently experiencing high tas will be hotter by 2045. These findings are consistent with many studies in the region and other parts of the world as result of the general warming reported by IPCC [1] [26].

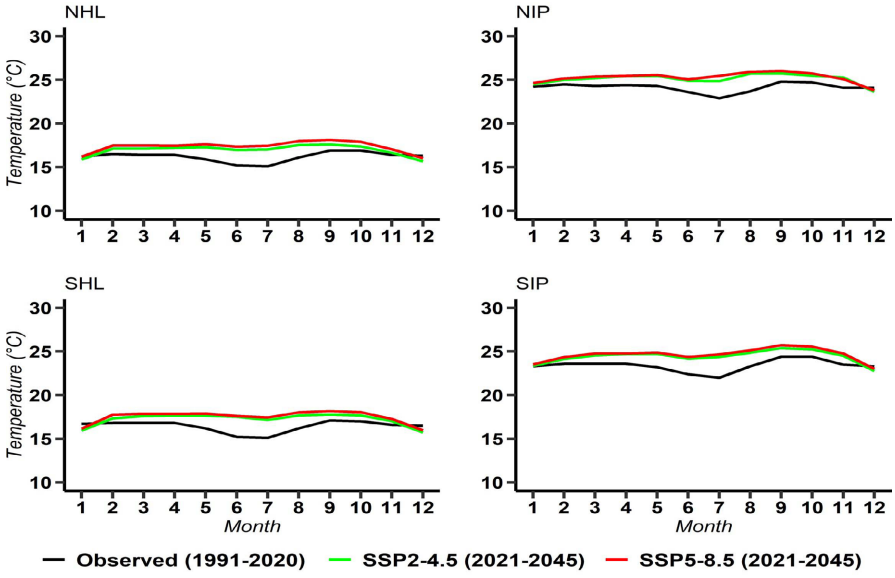

Figure 11. Projected monthly average temperature over the period 2021-2045.

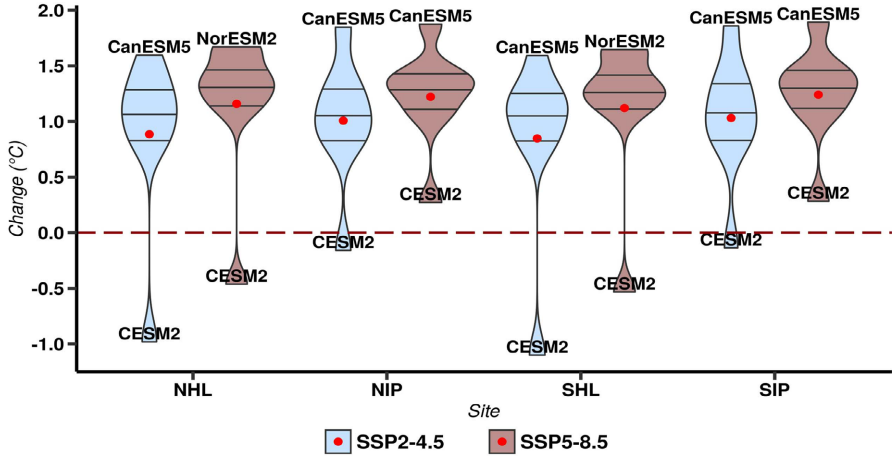

Figure 12. Projected changes in annual average temperature over the period 2021-2045.

3.2.3. Projected Wind Speed and Changes

Figure 13 depicts the projected monthly WS at NHL, NIP, SHL and SIP over the period 2021-2045 following SSP2-4.5 and SSP5-8.5.

The analysis revealed that a general increase in WS is expected from January to September all over the study area, while a decrease in WS is projected in November and December at NHL, NIP and SHL. The highest WS are projected in May-September with values more than 6 $m \cdot s^{-1}$ under both SSP2-4.5 and SSP5-8.5 all over the four sites. Actually, the analysis highlighted that WS forecasted under SSP5-8.5 are slightly higher during the long dry season than those under SSP2-4.5. In October, the findings do not predict any change in WS by 2045 under both scenarios all over the four sites. Indeed, the projected changes in WS will obviously have positive effect on wind energy production at NHL, NIP, SHL and SIP, especially in long dry season. On the other hand, **Figure 14** depicts average WS changes in quartiles. In fact, it is expected by 2045 an

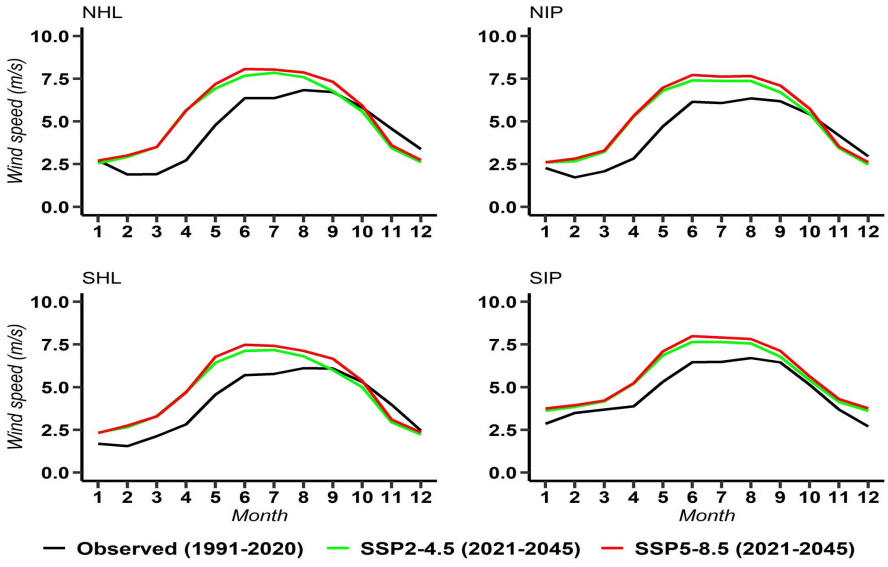

Figure 13. Projected monthly wind speed over the period 2021-2045.

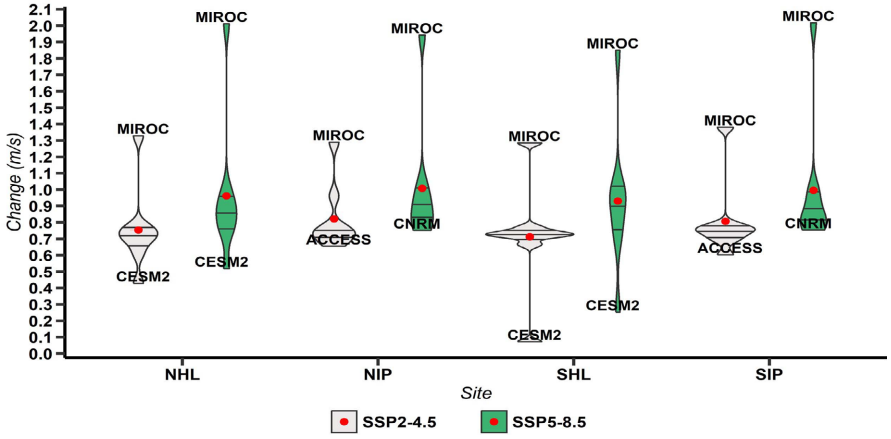

Figure 14. Projected changes in annual wind speed over the period 2021-2045.

average change in annual WS of 0.8 $m \cdot s^{-1}$ at NHL, NIP and SIP, and 0.7 $m \cdot s^{-1}$ at SHL under SSP2-4.5.

In SSP5-8.5, those average changes are projected to reach 1.0 $m \cdot s^{-1}$ at NHL, NIP and SIP, and 0.9 $m \cdot s^{-1}$ at SHL. Under both scenarios, the figure shows that MIROC projects maximum WS over the four sites, while CESM2 predicts minimum WS at NHL and SHL. At NIP and SIP, ACCESS and CNRM projects minimum WS under SSP2-4.5 and SSP5-8.5, respectively. Indeed, these findings highlighted that the four sites are only promising for installing wind turbine for small-scale power generation. Furthermore, the demand of water for irrigation is seasonal and our findings showed that the highest WS coincide with the long dry season which may favor drainage windmills. Otherwise, large-scale wind power require that mean WS exceed 7 $m \cdot s^{-1}$ to generate at least 200 $W \cdot m^{-2}$ [20].

3.2.4. Spatial Distribution of Changes

Figure 15 presents the spatial distribution of changes in annual rainfall over the

period 2021-2045. In both SSP2-4.5 and SSP5-8.5, the rainfall is expected to increase all over the study area with high values in the highlands than lowlands.

Indeed, at NHL and SHL, the increase in rainfall is especially predicted to be higher in the Center. Moreover, the forecasted increase in rainfall is expected be higher in SSP5-8.5 than SSP2-4.5. For instance in the Center of SHL, the increase in annual rainfall is expected to reach 100 mm under SSP2-4.5, while under SSP5-8.5 the increase is projected to reach 145 mm. Overall, these findings are in line with many other studies on precipitation around the globe as well as on East Africa [9] [21] [38]. **Figure 16** gives the spatial distribution of changes in annual tas over the period 2021-2045.

Under both SSP2-4.5 and SSP5-8.5, the tas is expected to increase all over the four sites. The analysis highlights that the increase under SSP5-8.5 is higher than SSP2-4.5. Actually, the spatial distribution of the predicted increase in tas is not homogeneous. In fact, the highest increase is expected at NIP, while the lowest increase is forecasted in the Center of NHL. Indeed, NIP and SIP which were hot under current climate are projected to be hotter. Overall, the general projected increase in tas found in this paper may be attributed to the global warming, and it is consistent with the findings by Brohan *et al.* [3] and many other studies around the globe on climate change. **Figure 17** depicts the future spatial distribution of changes in annual average WS.

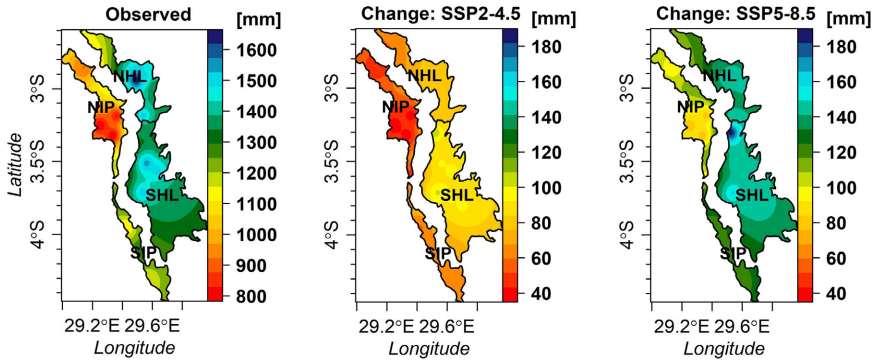

Figure 15. Observed (1991-2020) and spatial changes in annual rainfall over the period 2021-2045.

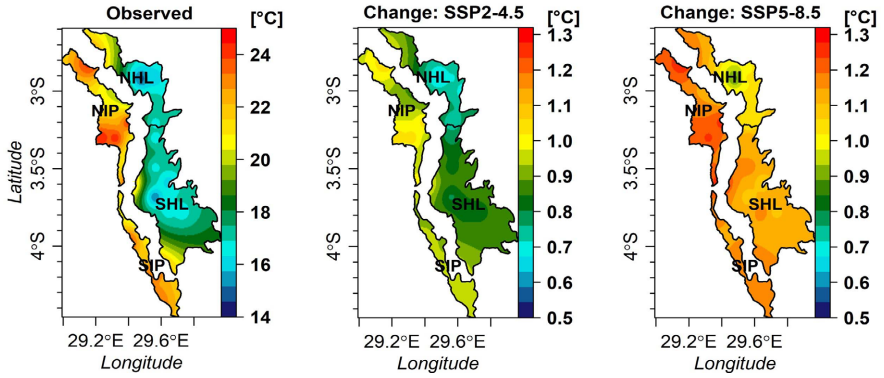

Figure 16. Observed (1991-2020) and spatial changes in annual tas over the period 2021-2045.

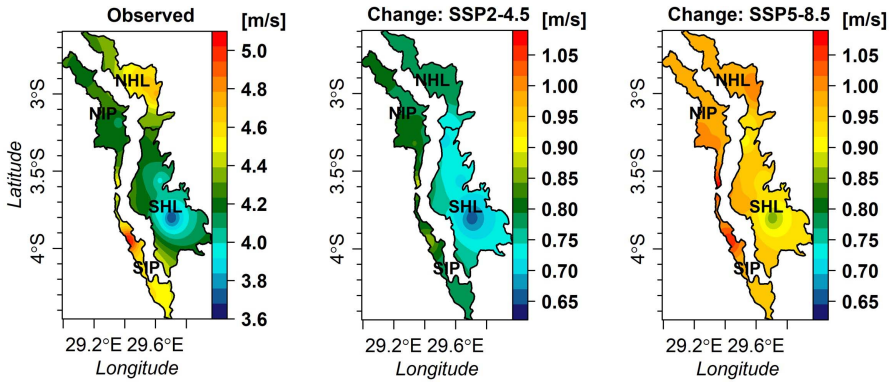

Figure 17. Observed (1991-2020) and spatial changes in annual WS over the period 2021-2045.

The analysis highlights that spatial distribution of projected changes in WS is not homogeneous. In fact, the sites NIP, NHL and SIP are expected to record the highest increase in WS, while the Center of SHL is predicted to experience the lowest. Actually, change values are slightly higher in SSP5-8.5 than SSP2-4.5. Overall, the findings revealed increase in projected WS; which is not a particular case for our study area. It is in accordance with other regional findings as well as studies around the globe [4] [40].

4. Conclusion

The study analyzed trends and changes in rainfall, tas and WS over the current period 1981-2020 and the future period 2021-2045 under SSP2-4.5 and SSP5-8.5. The characterization of the current period at monthly scales showed that June-September is in low rainfall over the period 1981-2020 except at NHL, where September is in excess rainfall. The months October-May were highlighted to be in excess rainfall all over the four sites. Using the MMK's test with TFPWMK approach over the period 1981-2010, a significant downward trend was revealed at NHL and SIP, while at NIP and SHL no significant downward trend was detected. Over the period 1981-2020, the Sen's slope estimated an upward trend at NHL, NIP and SHL, while a decreasing trend was estimated at SIP. Over the period 1991-2020, a significant increasing trend was revealed all over the four sites. On the other hand, an upward trend was found in tas all over the study area. Indeed, July was pointed out as the coolest month, while September is the hottest. Furthermore, an upward trend in WS was detected all over the four sites, and the highest monthly WS was found during the long dry season. Concerning the future trends, a general increase in rainfall, tas and WS is expected over the study area under both scenarios. In SSP2-4.5, rainfall changes of 5.9%, 4.7%, 6.5% and 5.1% are expected at NHL, NIP, SHL and SIP, respectively while in SSP5-8.5, these changes are projected to reach 10.2% at NHL, 9.7% at NIP, and 10.2% at SHL and SIP. For temperature, under SSP2-4.5, it is expected an average change of 0.8˚C at NHL and SHL, and 1˚C at NIP and SIP, while in SSP5-8.5, these changes will be equal to 1.1˚C at NHL and SHL, and 1.2˚C at NIP and SIP. On the other hand, under SSP2-4.5, it is projected an increase in

WS of 0.8 $m \cdot s^{-1}$ at NHL, NIP and SIP, and 0.7 $m \cdot s^{-1}$ at SHL. Meanwhile, under SSP5-8.5, these changes are expected to reach 1.0 $m \cdot s^{-1}$ at NHL, NIP and SIP, and 0.9 $m \cdot s^{-1}$ at SHL by 2045. The predicted increase in rainfall will have effects on water availability for hydropower production. It may also be translated in days with heavy rains. Likewise, the expected increase in WS may have a positive impact on wind power production, especially during the long dry season, or be used for water pumping in the irrigation system.

Acknowledgements

The authors gratefully acknowledge CHIRPS, CRU, MERRA-2, and CMIP6 for providing free access to their datasets. They also thank all other anonymous contributors.

Conflicts of Interest

The authors declare no conflicts of interest.

References

[1] IPCC (2007) Towards New Scenarios for Analysis of Emissions, Climate Change, Impacts and Response Strategies. IPCC Expert Meeting Report, Noordwijkerhout.

[2] Karl, T.R., Melillo, J.M. and Peterson, T.C. (2009) Global Climate Change Impacts in the United States. Cambridge University Press, Cambridge.

[3] Brohan, P., Kennedy, J.J., Harris, I., Tett, S.F.B. and Jones, P.D. (2006) Uncertainty Estimates in Regional and Global Observed Temperature Changes: A New Data Set from 1850. *Journal of Geophysical Research*, **111**, 106-126. https://doi.org/10.1029/2005JD006548

[4] Scott, E., James, M., Bart, N. and Wood, A. (2008) Climate Change Effects on Wind Speed. *North American Windpower*, **7**, 68-72.

[5] Yao, Y., Gordon, H.H. and Qianguo, L. (2012) Climate Change Impacts on Ontario Wind Power Resource. *Environmental Systems Research*, **1**, Article No. 2. https://doi.org/10.1186/2193-2697-1-2

[6] Shreck, C.J. and Semazzi, F.H.M. (2004) Variability of the Recent Climate of Eastern Africa. *International Journal of Climatology*, **6**, 681-701. https://doi.org/10.1002/joc.1019

[7] Laîné, A., Nakamura, H., Nishii, K. and Miyasaka, T. (2014) A Diagnostic Study of Future Evaporation Changes Projected in CMIP5 Climate Models. *Climate Dynamics*, **42**, 2745-2761. https://doi.org/10.1007/s00382-014-2087-7

[8] Buontempo, C., Mathison, C., Jones, R., Williams, K., Wang, C. and McSweeney, C. (2015) An Ensemble Climate Projection for Africa. *Climate Dynamics*, **44**, 2097-2118. https://doi.org/10.1007/s00382-014-2286-2

[9] Rowell, D.P., Booth, B.B., Nicholson, S.E. and Good, P. (2015) Reconciling Past and Future Rainfall Trends over East Africa. *Journal of Climate*, **28**, 9768-9788. https://doi.org/10.1175/JCLI-D-15-0140.1

[10] Vizy, E.K. and Cook, K.H. (2012) Mid-Twenty-First-Century Changes in Extreme Events over Northern and Tropical Africa. *Journal of Climate*, **25**, 5748-5767. https://doi.org/10.1175/JCLI-D-11-00693.1

[11] Cook, K.H. and Vizy, E.K. (2013) Projected Changes in East African Rainy Seasons.

Journal of Climate, **26**, 5931-5948. https://doi.org/10.1175/JCLI-D-12-00455.1

[12] DFID (2009) Economic Impact of Climate Change, Kenya, Rwanda, Burundi. ICPAC, Kenya and SEI Oxford Office, Nairobi.

[13] Ndayiragije, A., Mkezabahizi, D., Ndimubandi, J. and Kabogoye, F. (2017) A Scoping Study on Burundi's Agricultural Production in a Changing Climate and the Supporting Policies. Kenya Institute for Public Policy Research and Analysis, Nairobi.

[14] Bamber, P., Guinn, A. and Gereffi, G. (2014) Burundi in the Energy Global Value Chain: Skills of Private Sector Development. CGGC Duke University, Durham.

[15] Manirakiza, C., Lawin, A.E., Lamboni, B. and Niyongendako, M. (2021) Hydropower Potential in Near Future Climate over Burundi (East Africa): A Case Study of Rwegura Catchment. *Journal of Energy Research and Reviews*, **7**, 51-65. https://doi.org/10.9734/jenrr/2021/v7i130184

[16] Joel, N., Jackson, N. and Simon, M. (2014) Regional Flow Duration Curve Estimation and Its Application in Assessing Low Flow Characteristics for Ungauged Catchment. A Case Study of Rwegura Catchment-Burundi. *Nile Basin Water Sciences & Engineering Journal*, **4**, 14-23.

[17] Bidou, J.E., Ndayirukiye, S., Ndayishimiye, J.P. and Sirven, P. (1991) Géographie du Burundi (Geography of Burundi). Hatier, Paris.

[18] Lawin, A.E., Manirakiza, C. and Lamboni, B. (2019) Trends and Changes Detection in Rainfall, Temperature and Wind Speed in Burundi. *Journal of Water and Climate Change*, **10**, 852-870. https://doi.org/10.2166/wcc.2018.155

[19] Collins, C., Magnani, R. and Ngomirakiza, E. (2013) Food Security Country Framework for Burundi (FY 2014-FY 2019). USAID Office of Food for Peace, Washington DC.

[20] Manirakiza, C., Lawin A.E., Lamboni, B. and Niyongendako, M. (2019) Spatio-Temporal Analysis of Climate Change Impact on Future Wind Power Potential in Burundi (East Africa). *American Journal of Climate Change*, **8**, 237-262. https://doi.org/10.4236/ajcc.2019.82014

[21] Asfaw, A., Simane, B., Hassen, A. and Bantider, A. (2018) Variability and Time Series Trend Analysis of Rainfall and Temperature in Northcentral Ethiopia: A Case Study in Woleka Sub-Basin. *Weather and Climate Extremes*, **19**, 29-41. https://doi.org/10.1016/j.wace.2017.12.002

[22] Javier, E., Alba, L.-B.M., Carmen, C.-C., Amanda, P.G.-M., Ricard, K. and Raül, R.S. (2022) A Quality Control Procedure for Long-Term Series of Daily Precipitation Data in a Semiarid Environment. *Theoretical and Applied Climatology*, **149**, 1029-1041. https://doi.org/10.1007/s00704-022-04089-2

[23] Ioannis, Z. (2017) Combining Multiple Imputation with Cross-Validation for Calibration and Assessment of Cox Prognostic Survival Models. Leiden University, Leiden.

[24] Ayugi, B., Dike, V., Ngoma, H., Babaousmail, H., *et al.* (2021) Future Changes in Precipitation Extremes over East Africa Based on CMIP6 Models. *Water*, **13**, Article No. 2358. https://doi.org/10.3390/w13172358

[25] Kim, J.-B., Habimana, J.D.D., Kim, S.-H. and Bae, D.-H. (2021) Assessment of Climate Change Impacts on the Hydroclimatic Response in Burundi Based on CMIP6 ESMs. *Sustainability*, **13**, Article No. 12037. https://doi.org/10.3390/su132112037

[26] Almazroui, M., Saeed, F., Saeed, S., Islam, M.N., *et al.* (2020) Projected Change in Temperature and Precipitation over Africa from CMIP6. *Earth Systems and Envi-*

ronment, **4**, 455-475. https://doi.org/10.1007/s41748-020-00161-x

[27] Riahi, K., Van Vuuren, D., Kriegler, E., *et al.* (2017) The Shared Socioeconomic Pathways and Their Energy, Land Use, and Greenhouse Gas Emissions Implications: An Overview. *Global Environmental Change*, **42**, 153-168. https://doi.org/10.1016/j.gloenvcha.2016.05.009

[28] Iturbide, M., Gutierrez, J.M., Alves, L.M., *et al.* (2020) An Update of IPCC Climate Reference Regions for Sub Continental Analysis of Climate Model Data: Definition and Aggregated Datasets. *Earth System Science Data*, **12**, 2959-2970. https://doi.org/10.5194/essd-12-2959-2020

[29] Rasmus, E.B., Abdelkader, M. and Kajsa, M.P. (2015) ESD: Climate Analysis and Empirical-Statistical Downscaling (ESD) Package for Monthly and Daily Data.

[30] Cannon, A.J., Sobie, S.R. and Murdock, T.Q. (2015) Bias Correction of Simulated Precipitation by Quantile Mapping: How Well Do Methods Preserve Relative Changes in Quantiles and Extremes? *Journal of Climate*, **28**, 6938-6959. https://doi.org/10.1175/JCLI-D-14-00754.1

[31] Lawin, A.E., Manirakiza, C. and Lamboni, B. (2018) Wind Power Potential in Near Future Climate Scenarios: The Case for Burundi (East Africa). *Asian Journal of Environment & Ecology*, **8**, 1-10. https://doi.org/10.9734/ajee/2018/v8i430080

[32] McKee, T.B., Doesken, N.J. and Kleist, J. (1993) The Relationship of Drought Frequency and Duration to Time Scales. 8*th Conference on Applied Climatology*, Anaheim, 17-22 January 1993, 174-184.

[33] Mann, H.B. (1945) Nonparametric Tests against Trend. *Econometrica*, **13**, 245-259. https://doi.org/10.2307/1907187

[34] Kendall, M.G. (1962) Rank Correlation Methods. Hafner Publishing Co. Ltd., Royal Oak.

[35] Yue, S., Pilon, P., Phinney, B. and Cavadias, G. (2002) The Influence of Autocorrelation on the Ability to Detect Trend in Hydrological Series. *Hydrological Processes*, **16**, 1807-1829. https://doi.org/10.1002/hyp.1095

[36] Şen, Z. (2012) An Innovative Trend Analysis Methodology. *Journal of Hydrologic Engineering*, **17**, 1042-1046. https://doi.org/10.1061/(ASCE)HE.1943-5584.0000556

[37] Pettitt, A.N. (1979) A Non-Parametric Approach to the Change-Point Problem. *Journal of Applied Statistics*, **28**, 126-135. https://doi.org/10.2307/2346729

[38] Ongoma, V., Chena, H. and Gaoa, C. (2018) Projected Changes in Mean Rainfall and Temperature over East Africa Based on CMIP5 Models. *International Journal of Climatology*, **38**, 1375-1392. https://doi.org/10.1002/joc.5252

[39] George, Y.L. and David, W.W. (2008) An Adaptive Inverse-Distance Weighting Spatial Interpolation Technique. *Computers & Geosciences*, **34**, 1044-1055. https://doi.org/10.1016/j.cageo.2007.07.010

[40] Mahongo, S.B., Francis, J. and Osima, S.E. (2011) Wind Patterns of Coastal Tanzania: Their Variability and Trends. *Western Indian Ocean Journal of Marine Science*, **10**, 107-120.